

.....
Review
.....

Oriented Polycrystalline Oxide Ceramics Fabricated by Unidirectional Solidification of their Melts

Megumi TASHIRO, Tadashi KOKUBO, Setsuro ITO
and Masayuki ARIOKA*

Received October 25, 1975

The ceramics consisting of unidirectionally oriented crystals can be fabricated by unidirectional solidification of the oxide melts. They exhibit special features in a specific direction. The state of knowledge and understanding of the process of unidirectional solidification of the oxide melts, the microstructure of the resultant polycrystalline oxide ceramics, and their physical properties are reviewed. The results of investigation on the above subjects recently carried out in the authors' laboratory are incorporated in the present review.

I. INTRODUCTION

Ordinary ceramics are aggregates consisting of randomly oriented crystallites, and therefore are isotropic in property on the whole. The ceramics in which the constituent crystals were oriented unidirectionally during their fabrication process, however, possess special properties in a specific direction. Their anisotropy is governed not only by the degree of alignment of the crystallographic axis of their crystals but also by the degree of crystallographic anisotropy of the crystal themselves. Recently, the anisotropic ceramics have begun to attract considerable attention, and, actually, some of the ceramics recently developed show great excellence in mechanical, thermal, optical, electrical, or magnetic property in a specific direction.

There are three methods used for fabricating ceramics consisting of unidirectionally oriented crystals. They are, (a) to compact plate-like crystal grains so that their flat surfaces are arranged parallel, before or during sintering,¹⁻⁶⁾ (b) to crystallize a glass unidirectionally; *i.e.* successively from its one end to another,^{7,8)} and (c) to solidify a melt unidirectionally. Application of the methods (a) and (b) is limited; *i.e.* method (a) is applicable only to the raw materials, whose constituent crystal grains are of a special shape and method (b) only to the raw materials whose melts are likely to be supercooled as glass. Method (c), however, does not put any restriction on crystal shape or glass-forming ability of raw materials, and therefore are applicable to raw materials of broader systems.

Generally, oxide melt has much higher viscosity than that of metal melt, and, therefore, an ingot obtained by pouring an oxide melt into a mold is liable to contain many pores in its center. This is the reason why the method of casting melt has rarely been applied to the fabrication of polycrystalline oxides except for that of fusion-cast

* 田代 仁, 小久保正, 伊藤節郎, 有岡雅行: Laboratory of Ceramic Chemistry, Institute for Chemical Research, Kyoto University, Uji, Kyoto.

refractories in which the presence of pores are permissible if their location is restricted to the center of the ingot and their amount is not so large.⁹⁾ By method (c), a melt is solidified not from its all sides but unidirectionally; *i.e.* from its one end to the another successively, so that pores, even when formed at the crystal-melt interface, can rise up to the free surface of the melt. By this method, therefore, not only unidirectionally oriented polycrystalline ceramics but also those with markedly high density and, in an extreme case, with high optical transparency, can be obtained.

The purpose of the present article is to present the state of knowledge and understanding of the processes of unidirectional solidification of oxide melts as well as of the microstructures and properties of the resulting unidirectionally oriented polycrystalline oxide ceramics. The results of investigations on these subjects recently carried out in the authors' laboratory are described especially in detail.

II. METHODS OF UNIDIRECTIONAL SOLIDIFICATION OF MELT

Although some effective modifications were introduced, the methods presently used for fabricating unidirectionally oriented polycrystalline ceramics are almost the same as those hitherto used for fabricating a single crystal. They are: a) of Bridgman-type, b) of zone melting and c) of crystal pulling.

Noda *et al.*¹⁰⁾ used the Bridgman-type method for growth of book-type crystals of fluorine-containing mica. Although their studies were not aimed at fabricating a unidirectionally oriented polycrystalline aggregate, the results of their extensive works serve us as a good guide.

1. Bridgman-Type Method

A cylindrical crucible charged with a melt of raw materials is slowly lowered through a furnace with its long axis vertical, so that solidification of the melt begins from its bottom.

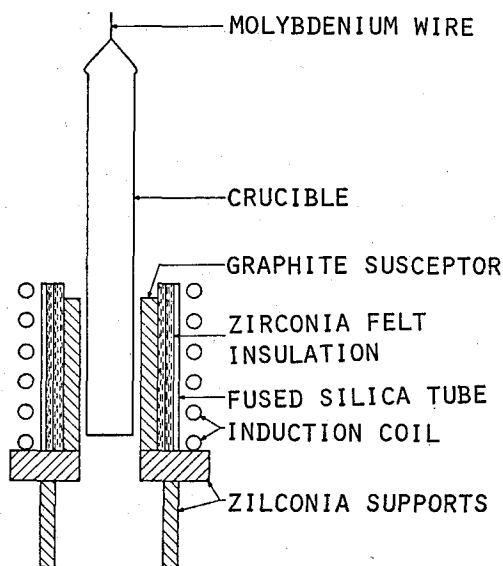


Fig. 1. An example of Bridgman-type apparatus used for fabricating unidirectionally oriented polycrystalline ceramics. (after Kennard *et al.*¹¹⁾)

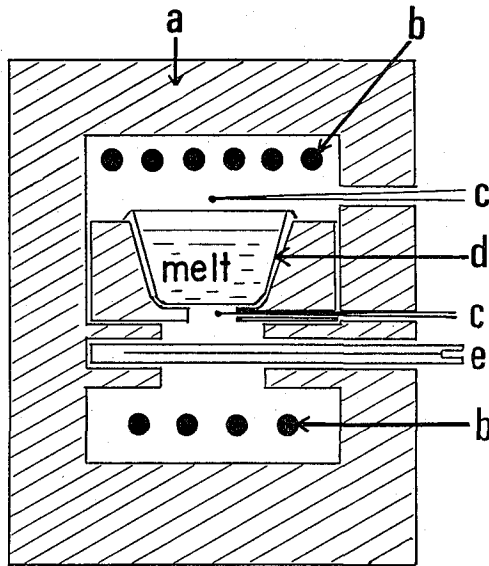


Fig. 2. An example of thermal gradient furnace for fabricating of unidirectionally oriented polycrystalline ceramics.¹⁸⁾
 a: Insulator, b: SiC heating elements, c: Thermocouple, d: Pt crucible,
 e: Water-cooled copper plate.

A crucible hitherto used for growth of a single crystal is sharpened to a point at its bottom so as to increase the chance that only one crystal will be formed. For growth of unidirectionally oriented polycrystallines, however, a crucible with a flat bottom, on which a large number of crystal nuclei are easily formed at the beginning of solidification of the melt, is used (Fig. 1¹¹⁾). When the crucible is lowered, many crystal nuclei are first formed, and then grow, forming a bundle of unidirectionally oriented columnar crystals. For the melt, whose nucleation rate is extremely low near its melting temperature, it is advisable to spread some crystals as seeds evenly at the bottom of the crucible. Usually, a Pt or Al_2O_3 crucible is used as a container for the compositions whose melting temperatures are below 1600°C .^{12,13)} A Pt or SiC resistance furnace is used for solidification of their melts. For the compositions with melting temperatures of $1600^\circ\text{--}2000^\circ\text{C}$, a molybdenum or tungsten crucible is used.^{11,14,15,16)} Their melts are solidified by using a r.f. induction furnace. In this case, the solidification must be performed in vacuum, or argon or helium gas atmosphere to prevent oxidation of the crucible.

When a big crucible is used, the use of an apparatus as shown in Fig. 2 is advisable.^{13, 17,18,19)} In the authors' laboratory an unidirectionally oriented crystalline aggregate of the composition, $0.7\text{NaNbO}_3 \cdot 0.3\text{BaTiO}_3$ (mol ratio), was obtained by the use of this apparatus.¹⁸⁾ An aggregate of this composition showed a strong quadratic electro-optic effect at room temperature. The process for its fabrication was as follows: A Pt crucible filled with the batch of this composition was heated from its top and bottom by applying an electric current through all of the SiC elements and kept at 1400°C . After the batch was melted completely, heating from the bottom was stopped and a water-cooled copper plate was inserted so that the melt was cooled from its bottom (Fig. 2). The electric current through the SiC elements placed above the crucible was kept flowing but slowly

decreased so that the temperature at the surface of the melt went down at a rate of $7^{\circ}\text{C}/\text{hr}$. By this procedure the melt was solidified from its bottom at a rate of $1\text{ mm}/\text{hr}$. The temperature difference between the upper surface and bottom of the melt was kept constant, *i.e.* at about 300°C until the whole of the melt was solidified. The ingot thus obtained was taken out from the platinum crucible by tapping its outer surface with a plastic hammer.¹⁹⁾

The big advantages of the Bridgman-type method is its capability of fabricating a crystalline aggregate of a fairly large size. By this method even a melt with a high vapor pressure can be solidified without weight loss if the crucible is sealed tightly with a lid. Its disadvantages are as follows: a) Since this method necessitates the use of a container, the melt to be solidified is liable to be contaminated with the components of the container. b) When the ingot is cooled to room temperature, a fairly large mechanical stress is induced in it because of the big difference in thermal expansion coefficient between the ingot and crucible. Under this stress minute cracks are liable to form in the ingot. c) In order to precipitate long columnar crystals unidirectionally arranged from the melt and also to prevent any type of segregation between the crystals during solidification of the melt, application of a steep temperature gradient in the direction of solidification to the melt adjacent to the crystal-melt interface is necessary.²⁰⁾ By the Bridgman-type method, however, it is not easy to set up such a condition, especially in the case when the melt to be solidified is oxide, because an oxide phase precipitated generally has a much lower thermal conductivity compared to that of metal, acts as a layer of thermal insulator during the solidification process, and thus lowers the temperature gradient in the melt adjacent to the crystal-melt interface. The temperature gradient hitherto achieved by this method for solidification of oxide melts is reported to be $80\text{--}220^{\circ}\text{C}/\text{cm}^{11\text{--}19)$ which is much lower than those achieved by the other methods to be described in the following.

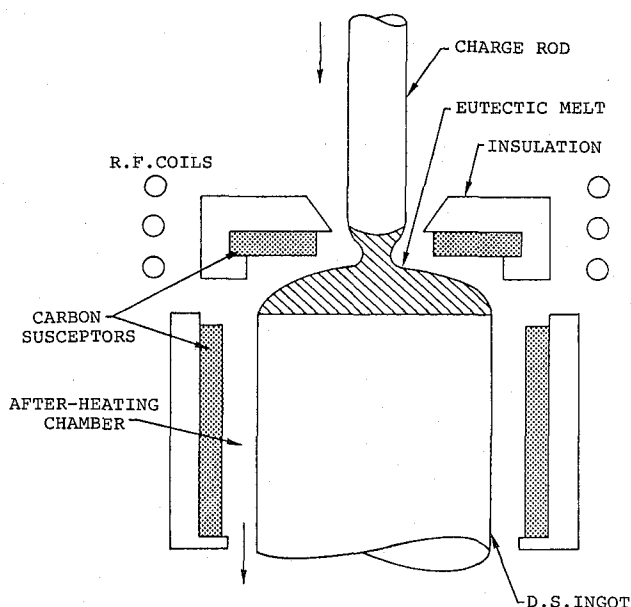


Fig. 3. An example of zone melting apparatus for fabricating unidirectionally oriented polycrystalline ceramics. (after Hulse *et al.*¹⁹⁾)

2. Zone Melting Method

This method is similar in principle to that widely used for purifying crystals or for fabricating a single crystal. It has been applied to fabricating unidirectionally oriented polycrystalline aggregates, mainly, of the eutectic compositions such as $\text{Al}_2\text{O}_3\text{-ZrO}_2$ (Y_2O_3),^{13,21)} $\text{ZrO}_2\text{-Y}_2\text{O}_3$,¹³⁾ $\text{CaO}\cdot\text{ZrO}_2\text{-ZrO}_2$,¹³⁾ MgO-CaO ,¹³⁾ $\text{BaFe}_{12}\text{O}_{19}\text{-BaFe}_2\text{O}_4$,²²⁾ $\text{Al}_2\text{O}_3\text{-TiO}_2$,²³⁾ NiO-CaO ²⁴⁾ etc.. As an example, a device used for fabricating the $\text{Al}_2\text{O}_3\text{-ZrO}_2(\text{Y}_2\text{O}_3)$ polycrystalline aggregate is schematically shown in Fig. 3.¹³⁾ Powders of the raw materials are compacted into a rod by sintering or fusion-casting. The rod thus formed is lowered slowly through a r.f. induction furnace, first to melt a short zone of the bar, and then to pass the molten zone along the bar. If the lower part of the bar is pulled downward at a lower rate than that of the upper part not yet molten, the resulting rod will be thickened as shown in Fig. 3. The rod thus obtained consists of columnar crystals unidirectionally oriented along the axis of the rod.

For heating a short zone of the bar, resistance heaters,^{13,21)} electron beams²³⁾ or arc images²⁴⁾ can also be used.

Since this method does not necessitate the use of a crucible, there is no possibility for the melt to be contaminated with the components of the crucible and, therefore, a composition with a high melting temperature can easily be processed by this method. Furthermore, there is no possibility of development of cracks in the product caused by the difference in thermal expansion coefficient between the crucible and the ingot. The most important advantage of this method is that by this method a steep temperature gradient can be applied to the melt adjacent to the crystal-melt interface, which is most necessary for forming long columnar crystals in an orderly unidirectional array without causing any type of segregation between the crystals. The maximum temperature gradient hitherto achieved for solidification of oxide melts is reported to be $2000^\circ\text{C}/\text{cm}$.¹³⁾ One of the big disadvantages of this method is a difficulty in obtaining an ingot a with big diameter.

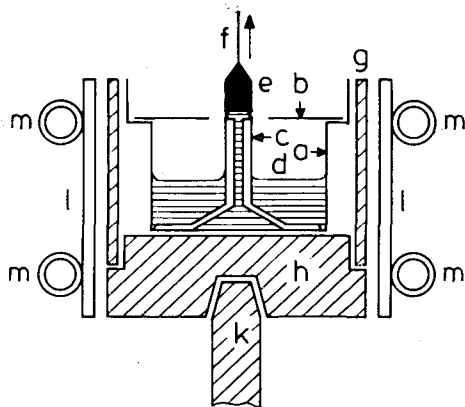


Fig. 4. An example of apparatus for pulling unidirectionally oriented polycrystalline ceramics. (after Boomgaard *et al.*²⁵⁾)

a: Pt 30% Rh crucible, b: Lid of the same material, c: Cappillary of the same material o.d. 5 mm, i.d. 0.8 mm, d: Melt, e: Growing composite material, f: Pt 20% Rh wire, g: Ceramic ring, h: Ceramic plate, k: Ceramic rod, l: Copper r.f. coil, m: Water cooling (copper pipe).

3. Crystal Pulling Method

As an example, the apparatus used for solidifying the melt of the system, $\text{BaTiO}_3\text{--}(\text{CoFe}_2\text{O}_4)_{1-x}(\text{Co}_2\text{TiO}_4)_x$, into a unidirectionally oriented polycrystalline aggregate is schematically shown in Fig. 4.²⁵⁾ The melt was pulled through a Pt20–30Rh capillary placed in the center of the melt to be formed into a rod of unidirectionally oriented polycrystalline aggregate. The diameter of the solidified rod is determined by the diameter of the platinum capillary as well as the pulling rate. By changing the shape of the cross-section of the capillary, polycrystalline aggregates with various shapes such as tubular shape can be fabricated.^{26,27)} Similarly to the zone melting method, no mechanical stress is induced in the solidified rod in this process because the melt solidifies freely without adhering to the wall of the crucible. Disadvantages of this method are that a) the melt is liable to be contaminated by the components of the crucible or capillary materials, b) a melt with a high vapor pressure can not be processed since the crucible can not be covered tightly with a lid.

III. MICROSTRUCTURE OF POLYCRYSTALLINE AGGREGATES

The polycrystalline aggregates fabricated by the unidirectional solidification of their melts are mainly composed of columnar crystals. Their size, shape, and orientation are governed by the chemical composition of the melt and condition of its solidification. The compositions of the melts hitherto solidified by the three methods described in the preceding chapter, are limited mostly to the congruently melting compositions and eutectic composition. Among the three methods the Bridgman-type method has been used most frequently. In the followings, therefore, the discussion will be confined mostly to the microstructures of the polycrystalline aggregates obtained by the Bridgman-type method.

1. Diameter of Columnar Crystals and their Orientation

At the beginning of the unidirectional solidification of a melt, nuclei formed at the bottom of the melt start to grow individually to various directions crystallographically favorable for each of the crystals, forming a layer of randomly oriented crystals. When the nuclei are densely formed, crystals originating from the nuclei soon hit each other and only the crystals whose favorable orientations are close to the direction of the temperature gradient survive, resulting in formation of an aggregate of unidirectionally oriented

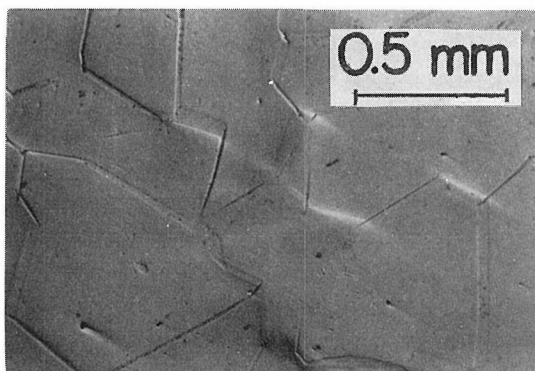


Fig. 5. Transverse section of 0.7 $\text{NaNbO}_3\cdot 0.3 \text{BaTiO}_3$ solidified ingot (Transmitted light).¹⁸⁾

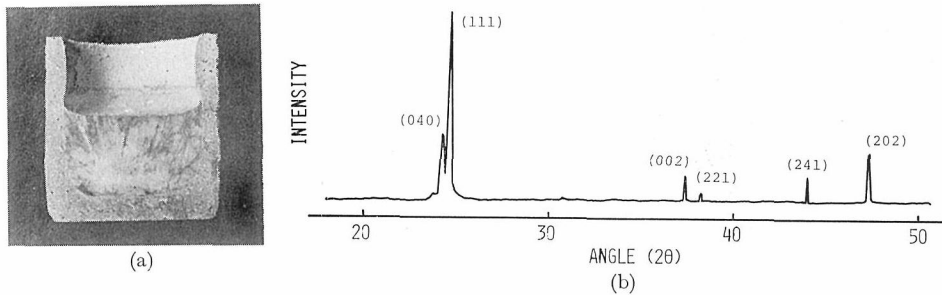


Fig. 6. (a) Longitudinal section of $\text{Li}_2\text{O}\cdot 2\text{SiO}_2$ solidified ingot.¹⁹⁾ (b) X-ray diffraction pattern of a transverse section of the same ingot.¹⁹⁾

columnar crystals.²⁸⁾ This was actually the case for the melt of the $0.7\text{NaNbO}_3\cdot 0.3\text{BaTiO}_3$ composition described in the forgoing chapter. When it was solidified unidirectionally at a rate of 1 mm/hr (a rate of movement of the crystal-melt interface), a layer about 0.5 mm thick consisting of randomly oriented crystals of the perovskite-type was first formed in the melt adjacent to the bottom of the crucible. On further solidification, only the crystals whose $\langle 110 \rangle$ direction was close to the direction of the temperature gradient kept growing, without hitting each other, forming an array of unidirectionally oriented columnar crystals. The diameter of the columnar crystals grown at a rate of 1 mm/hr was 0.5 mm. Figure 5 shows a transverse section of a portion of the unidirectionally oriented crystalline aggregate thus obtained.

In the melts containing glass-forming oxides, however, nucleation is difficult to occur on its cooling. When such a melt is solidified unidirectionally, few nuclei is formed and the nuclei formed sparsely in the melt at the bottom of the crucible grow radially to a fairly long distance without hitting each other. Figure 6 shows, as an example, the microstructure formed by such a mechanism; a batch of the $\text{Li}_2\text{O}\cdot 2\text{SiO}_2$ (mol ratio) composition was melted completely in a clay crucible, and the melt was solidified unidirectionally from its bottom at a rate of 3.3 mm/hr. As can be seen from the photograph of the longitudinal section of the ingot and the X-ray diffraction pattern from its transverse section, crystal columns originating from a few spots at the bottom of the crucible are not arrayed unidirectionally in the direction of the solidification but a little inclined, developing a part of the radial pattern. The diameter of the crystal columns was big and uneven.

In order to enhance nucleation in such a melt, it is advisable to spread, on the bottom of the crucible, a layer of crystal seeds, if possible, of the same composition as that of the melt to be solidified. As a pretreatment for unidirectional solidification of the $\text{Li}_2\text{O}\cdot 2\text{SiO}_2$ melt, the present authors formed such a layer of crystal seeds using a technique used for fabricating glass-ceramics;¹⁹⁾ a small amount of melt of the $\text{Li}_2\text{O}\cdot 2\text{SiO}_2$ composition was spread on the bottom of the crucible to form a thin glassy layer about 2 mm thick, which by a successive heat treatment at 900°C was converted to an aggregate of the $\text{Li}_2\text{O}\cdot 2\text{SiO}_2$ crystallites. The crystallites formed at the upper free surface of the crystallized glass layer were found to be of a columnar shape of about $10\ \mu\text{m}$ in diameter, being oriented with their $\langle 001 \rangle$ direction perpendicular to the free surface of the layer.¹⁹⁾ Into this pretreated crucible, a melt of the same composition, *i.e.* $\text{Li}_2\text{O}\cdot 2\text{SiO}_2$, which had been well degassed by refining for a long period in another crucible, was poured, followed by the usual Bridgman-type process as described in the preceding chapter. The ingot thus

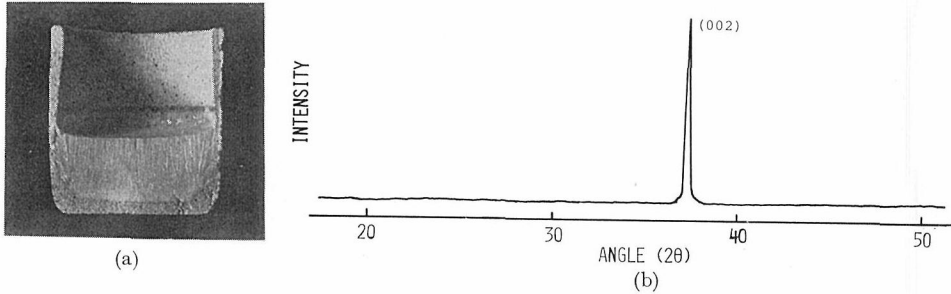


Fig. 7. (a) Longitudinal section of $\text{Li}_2\text{O}\cdot 2\text{SiO}_2$ ingot solidified on a $\text{Li}_2\text{O}\cdot 2\text{SiO}_2$ glass-ceramic layer.¹⁹⁾ (b) X-ray diffraction pattern of transverse section of the same ingot.¹⁹⁾

obtained consisted of columnar crystals of the $\text{Li}_2\text{O}\cdot 2\text{SiO}_2$ composition oriented unidirectionally in the direction of solidification. The diameter of each of the columnar crystals was about $200\ \mu\text{m}$ when the crystals grew at a rate of $3.3\ \text{mm/hr}$. The photograph of a longitudinal section of the ingot and the X-ray diffraction pattern from its transverse section are shown in Figs. 7 (a) and (b), respectively.

The diameter of each of the columnar crystals in the ingot appeared to decrease with increasing number of the crystal nuclei artificially spread or spontaneously developed on the bottom of the crucible and also with increasing rate of solidification (rate of movement of the crystal-melt interface). Their relations, however, have not yet fully been exploited. For metals of eutectic compositions,²⁹⁾ the following relation exists between the interlamellar spacing λ and the solidification rate R_s .

$$\lambda^2 \cdot R_s = \text{const.}$$

Kennard *et al.*^{11,13,16,23)} have confirmed that this relation also exists for the eutectic oxide melts. This relationship is shown, for example, in Fig. 8.

2. Crystal Face

According to Jackson *et al.*³⁰⁾ the face of the crystals growing in the melt of the congruently melting composition is strongly dependent on the entropy of melting,

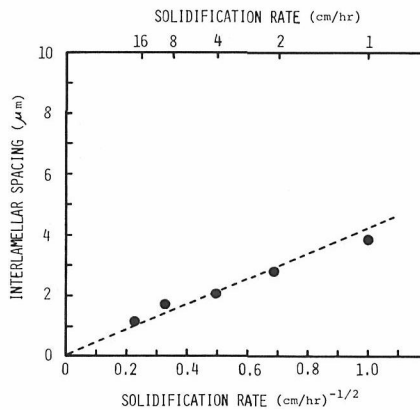


Fig. 8. Interlamellar spacing *vs* inverse square root of solidification rate. Composition: $\text{ZrO}_2\text{-MgO}$. (after Kennard *et al.*¹⁶⁾)

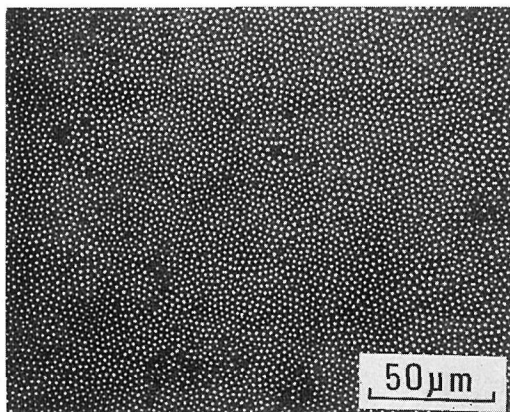


Fig. 9. Transverse section of $\text{Fe}_2\text{O}_3\text{-LaFe}_{12}\text{O}_{19}$ eutectic solidified ingot (Transmitted light). (after Hulse *et al.*¹³⁾)

$\Delta H_f/T_e$, where ΔH_f is the molecular heat of melting and T_e is the melting temperature: The materials having high entropies of melting (greater than $2R$) grow with crystalline facets and those having low entropies of melting (less than $2R$) grow almost isotropically with no facets. Since most oxides have high entropies of melting, it is naturally expected that the constituent columnar crystals of the aggregate solidified unidirectionally from the melt of the $\text{NaNbO}_3\text{-BaTiO}_3$ composition described in the preceding section would also have faceted faces. This is actually demonstrated in the micrograph shown in Fig. 5. Jackson *et al.*³⁰⁾ proposed further that a crystalline aggregate solidified from the melt of the eutectic composition has a regular structure, such as lamellar or rod-like structure, only when both phases of the eutectic have low entropies of melting or when only one has high entropies of melting. On the basis of Jackson's proposal, it was once concluded that the oxide eutectic having a regular structure was difficult to be solidified from the oxide melt, since both phases of the oxide eutectic usually have high entropies of melting.¹²⁾ Recently, however, it was found experimentally that regular structures were formed even in the oxide eutectics in which both phases have high entropies of melting.^{11,14~16,21~25)} An example of such regular structures is shown in Fig. 9.¹³⁾ For oxide eutectics, regularity of the eutectic structures might be determined not only by the entropy of melting but also some other factors such as the temperature gradient in the melt adjacent to the crystal-melt interface during solidification.¹⁴⁾

3. Length of Columnar Crystal

Whether columnar crystals continue or intermit to grow in the melt during its unidirectional solidification is determined mainly by the variation in amount of undercooling ΔT of the melt in the direction of solidification. When the pure oxide melt of the congruently melting composition is solidified unidirectionally from its one end at a slow rate, the temperature distribution near the crystal-melt interface is represented schematically by a dotted line in Fig. 10 (a). A solid line drawn in the same figure represents the temperature distribution at the condition for stationary interface. As can be seen from the figure, the amount of supercooling ΔT is the biggest at the interface, decreasing with increasing distance from the interface in the direction of solidification. Consequently,

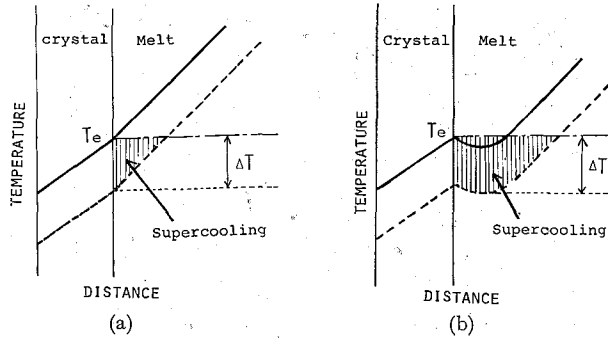


Fig. 10. Temperature profile near crystal-melt interface. (a) Congruently and slow solidification. (b) Congruently and rapid solidification. T_e : Melting temperature, ΔT : Supercooling.

the front of the crystal phase can continue to advance with a planar surface, and thus the crystalline aggregate, in which long columnar crystals are unidirectionally oriented, can be obtained.

When the same melt is solidified rapidly, a part of the latent heat evolved by solidification is accumulated at the interface, resulting in change of the temperature gradient in the melt from positive to negative as shown by the dotted line drawn in the left side of Fig. 10 (b). In this case, the amount of supercooling ΔT in the melt increases with increasing distance from the interface in the direction of solidification. When a random protuberance of the crystal phase arises under this condition, it extends into a portion of the melt where ΔT is larger, forming a filamented crystal. In an extreme case, a new crystal nucleus is formed in a portion of the melt far off from the main interface where ΔT is much larger, forming an solitary crystal island. In these cases, a continuous cellular structure or partly broken cellular structure is formed at the front of the crystal phase as shown in Fig. 11 (a) or Fig. 11 (b). The length of cellular crystals becomes shorter as the negative temperature gradient in the melt near the interface is set steeper.

The maximum supercooling in a portion of the melt far apart from the interface also occurs when the composition of the melt deviates from its initial congruently melting composition by some reasons such as contamination of impurities or vaporization of a part of the constituents of the melt during solidification. This compositional deviation changes the mechanism of solidification from of the pure liquid type to of the solid solution type, causing a so-called constitutional supercooling in the melt near the crystal-melt interface:²⁰ When a melt of initial composition C_0 is solidified unidirectionally, the compositions of the melt and the crystal phase both adjacent to the advancing crystal-melt

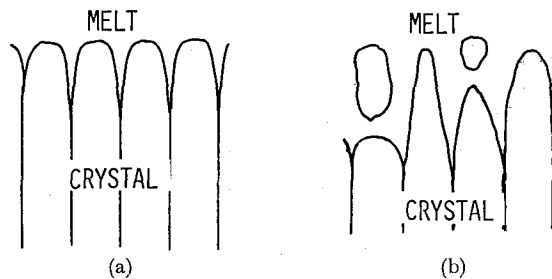


Fig. 11. Cellular structure.

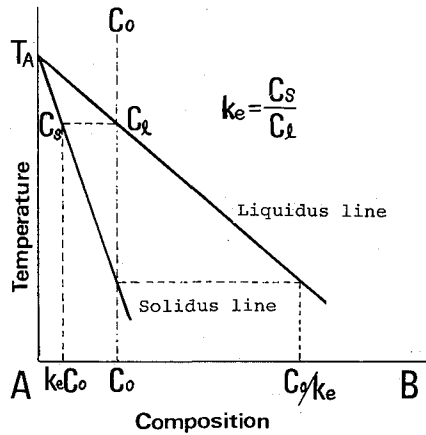


Fig. 12. An example of phase diagram.

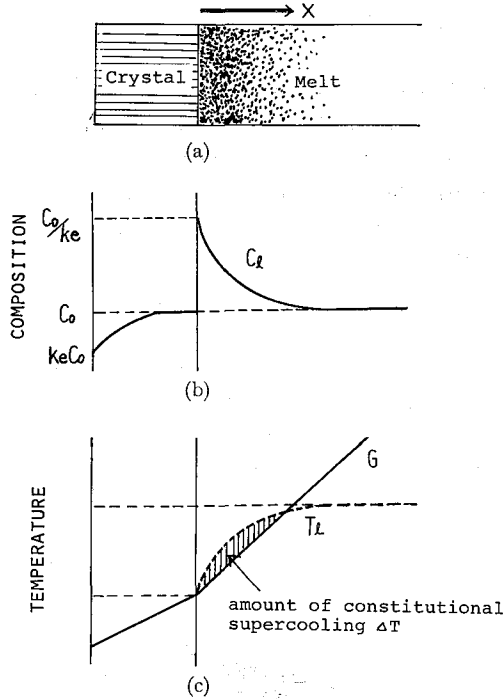


Fig. 13. Constitutional supercooling in incongruently solidification.
 (a) (b): Solute profile. (c): Temperature profile.

interface follow the liquidus ($C_0 \rightarrow C_0/k_e$) and solidus ($k_e C_0 \rightarrow C_0$) lines, respectively (Fig. 12). Figure 13 (b) shows a profile of composition at the time when the composition of the melt adjacent to the interface reaches C_0/k_e . In Fig. 13 (c) a dotted line, T_L , shows the distribution of the equilibrium liquidus temperature of the melt, and a solid line, G , shows the actual temperature distribution. The amount of the supercooling ΔT is represented by the difference between the actual temperature and the liquidus temperature. The amount of constitutional supercooling increases with increasing distance

from the solid-liquid interface until it passes through the maximum. This variation is alike to that shown in Fig. 10 (b). This means that the crystals growing in the melt during its unidirectional solidification also take the cellular form and their length becomes shorter when the composition of the melt deviates from its original congruently melting composition.

The requirement for each crystal to grow continuously without taking the cellular from or its breaking during unidirectional solidification is that no region of constitutional supercooling exists ahead of the crystal-melt interface. This condition²⁰⁾ is expressed by

$$G = dT/dx > \{mC_0R_s/D\} \{(1-k_e)/k_e\}$$

where $G = dT/dx$ is the actual temperature gradient, T is the actual temperature, x is the distance from the crystal-melt interface, m is the slope of the liquidus curve, R_s is the rate of movement of the interface, D is the diffusion coefficient for the solute in the melt, C_0 is the initial composition of the melt (Fig. 12), k_e is an equilibrium partition ratio, $k_e = C_s/C_l$, where C_s and C_l are the crystal and melt compositions, respectively, being fixed by the phase diagram.

4. Segregation

When the composition of the melt deviates from its initial congruently melting composition by some reasons described in the preceding section, the components excessive for its congruently melting are rejected at the crystal-melt interface during solidification, and remain at the boundaries between the cellular crystals. Figures 14 and 15 show an example of segregation caused by the mechanism described above: Figure 14 is the micrograph of a longitudinal section of an aggregate of columnar crystals grown in the melt of the composition 0.7 NaNbO₃·0.3 BaTiO₃ using the apparatus as shown in Fig. 2. The temperature gradient applied to the melt adjacent to the interface was 70°C/cm and the rate of movement of the interface was 1 mm/hr. This composition is originally of the congruently melting.³¹⁾ During solidification, however, the components, Na₂O and Nb₂O₅, although in a small amount, vaporized from the melt, causing a deviation of the composition from of congruently to of incongruently melting. As the result, some constituents excessive in amount for the congruently melting composition were segregated from the melt, precipitating at the deep grain boundary grooves of a bundle of the 0.7Na-NbO₃·0.3BaTiO₃ crystals as shown in Fig. 14.¹⁸⁾ Figure 15 shows the existence of foreign

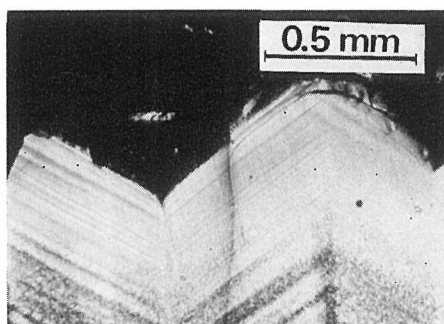


Fig. 14. Longitudinal section of columnar crystals growing in 0.7 NaNbO₃·0.3 BaTiO₃ melt. The bulk liquid was decanted in the middle of solidification.¹⁸⁾

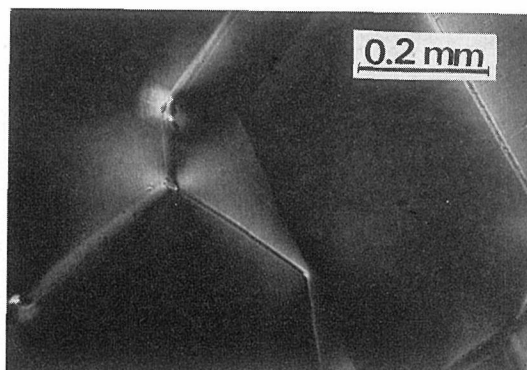


Fig. 15. Transverse section of $0.7 \text{ NaNbO}_3 \cdot 0.3 \text{ BaTiO}_3$ solidified ingot showing some inclusions among the major crystals (Transmitted light with crossed nicols).¹⁸⁾

materials segregated at the boundaries of the $0.7\text{NaNbO}_3 \cdot 0.3\text{BaTiO}_3$ faceted crystals especially at the corners where three crystals meet together.

5. Porosity

When an oxide melt is poured into a cold mold, solidification proceeds from its all sides, resulting in formation of many big cavities in the central part of the ingot. This is due to the volume shrinkage of the melt occurring on its solidification.³¹⁾ Formation of such big cavities can be avoided by solidifying the melt unidirectionally. Even when the melt is solidified unidirectionally, however, it is not easy to suppress the formation of tiny pores in the ingot. When a melt containing a gas in solution solidifies, gas is rejected at the crystal-melt interface. The gas rejected can reach a free surface of the melt either by diffusing in the melt or by the formation of a gas bubble which rises upwards. If the escaping rate of the gas by these mechanisms is low relative to the advancing rate of the crystal-melt interface, the gas bubbles evolved at the interface are trapped by the advancing crystal phase, remaining in it as pores. If the escaping rate of the gas is high relative to the advancing rate of the interface, no pores are formed in the crystal phase. The former case is likely to occur for the oxide melts, whose viscosity is high even at their melting temperature. The latter case is likely to occur for the metal melts whose viscosity is low at their melting temperature.

The $0.7\text{NaNbO}_3 \cdot 0.3\text{BaTiO}_3$ melt described above has a low viscosity at its melting temperature, and, consequently, corresponds to the melt in the latter case: By solidifying the melt at a rate of 1 mm/hr, a micropore-free highly dense crystalline aggregate consisting of unidirectionally oriented crystals of the above composition can easily be obtained as shown in Fig. 5.¹⁸⁾

The $\text{Li}_2\text{O} \cdot 2\text{SiO}_2$ melt described in the foregoing has a high viscosity at its melting temperature because it contains a glass-forming oxide, and consequently, corresponds to the melt in the former case, in which the gas bubbles evolved are likely to be trapped by the advancing crystal phase. In the viscous melt, transport of gas away from the interface by diffusion is not sufficiently high to hold the gas in solution in the melt, and then the gas is evolved as bubbles. Since the solid-liquid interface does not act as an effective nucleant³²⁾ for the formation of gas bubbles, nucleation of bubbles would occur in the melt

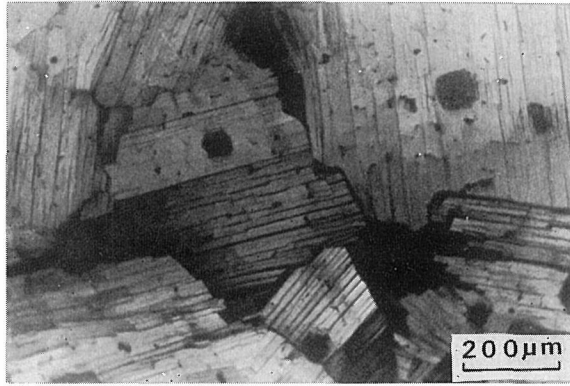


Fig. 16. Pores formed in $\text{Li}_2\text{O}\cdot 2\text{SiO}_2$ ingot solidified at a rate of 3.3 mm/hr (Transverse section observed with transmitted light).¹⁹⁾

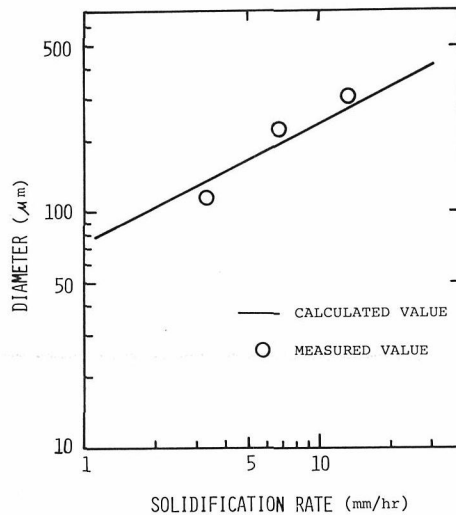


Fig. 17. Solidification rate dependence of maximum diameter of pore formed in solidified $\text{Li}_2\text{O}_3\cdot 2\text{SiO}_3$ ingot.¹⁹⁾

a little apart from the interface but not by contact with the interface. A gas nucleus thus formed grows in size, rising up in the melt at a rate³³⁾ of

$$R_f = (1/12)d^2g\rho/\eta$$

where d is the diameter of the bubble, g is the acceleration of gravity, ρ is the density of the melt and η is its viscosity. If the solidification rate (rate of movement of the interface) is higher than the R_f value for the bubble, the bubble is trapped by the front of the crystal phase, remaining as a micropore. For example, micropores formed in an ingot by such a mechanism is shown in Fig. 16. The ingot was obtained by solidifying the $\text{Li}_2\text{O}\cdot 2\text{SiO}_2$ melt unidirectionally at a rate of 3.3 mm/hr.¹⁹⁾ Figure 17 shows a relation between the solidification rate and the maximum diameter of the pores formed in each of the ingots solidified from the $\text{Li}_2\text{O}\cdot 2\text{SiO}_2$ melt at various solidification rates. A solid line represents the relation obtained from the above equation. It can be seen from the figure that the

experimental data are in good agreement with the values calculated.¹⁹⁾

IV. PROPERTIES OF UNIDIRECTIONALLY SOLIDIFIED POLYCRYSTALLINE CERAMICS

1. Densification

Dense polycrystalline ceramics having almost zero porosity can be fabricated fairly easily by the unidirectional solidification under proper fabricating conditions. The fabrication of ceramics of the $\text{NaNbO}_3\text{-BaTiO}_3$ system having almost zero porosity described in the preceding chapter is one of the examples. The porosity of the ceramics of this system hitherto achieved by the conventional sintering method was 20%.³⁴⁾

Some polycrystalline ceramics having extremely low porosity show high optical transparency. Combination of their optical transparency with their another special property would give the promise of their future unique use. For example, the transparent polycrystalline ceramics of the $0.7\text{NaNbO}_3\cdot 0.3\text{BaTiO}_3$ composition fabricated by the unidirectional solidification method is promising for use as a quadratic electro-optic material. The as-solidified ingot of this composition, however, is dark-blue. For its decoloration, it must be reheated at 800°C for more than 10 hr, after sliced into thin plate of 0.1–1.0 mm in

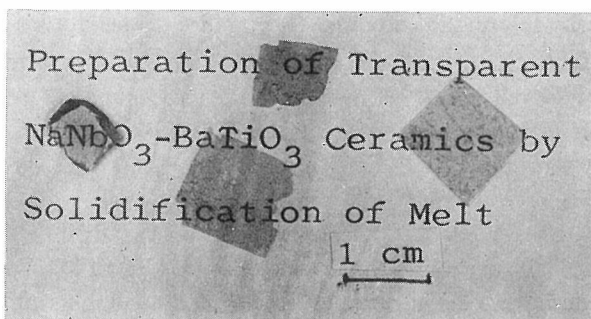


Fig. 18. Thin transverse section of $0.7 \text{NaNbO}_3\cdot 0.3 \text{BaTiO}_3$ solidified ingot.¹⁸⁾

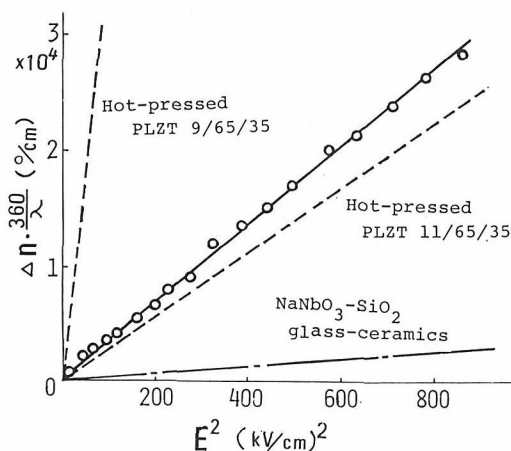


Fig. 19. Birefringence of $0.7 \text{NaNbO}_3\cdot 0.3 \text{BaTiO}_3$ solidified ingot induced by applied electric field.³⁵⁾

thickness. Figure 18 shows the transparent thin sections, 0.1–1.0 mm thick, of the ingot cut transversely to the direction of its solidification. When the electric voltage was applied on their both sides, these sections showed a strong birefringence proportional to the square of the applied voltage as shown in Fig. 19.³⁵⁾ The data for a glass-ceramic of the $\text{NaNbO}_3\text{-SiO}_2$ system³⁶⁾ and various kinds of hot-pressed PLZT³⁷⁾ hitherto reported are reproduced in the same figure for comparison. For fabricating the transparent PLZT ceramics, it is necessary to sinter their raw materials under high pressure³⁷⁾ or in the well controlled gas atmosphere.³⁸⁾

2. Anisotropy

Unidirectionally solidified ceramics have special properties in a specific direction.

Harrion¹²⁾ reported that crystalline aggregates solidified unidirectionally from the melt of an eutectic composition in the $\text{ZnO-B}_2\text{O}_3$ system show a specific resistivity of 10^{10} Ωcm in a direction of their solidification and 10^{12} Ωcm in a direction perpendicular to the solidification, and therefore they can be utilized as a high-impedance current divider. Hulse *et al.*^{13,21)} reported that crystalline aggregates solidified unidirectionally from the melt of an eutectic composition in the $\text{Fe}_2\text{O}_3\text{-LaFe}_{12}\text{O}_{19}$ system has a structure in which the needle-like $\text{LaFe}_{12}\text{O}_{19}$ crystals with their major axis parallel to the direction of their solidification are distributed uniformly in the Fe_2O_3 matrix, and therefore they can be used as a high density information storage. The ability of the whiskers of $\text{LaFe}_{12}\text{O}_{19}$ to transmit polarized light perpendicular to the transverse section depends upon their direction of magnetization. Terrell *et al.*^{25,39)} obtained the crystalline aggregates showing a magneto-electric effect by unidirectional solidification of the melts of the eutectic compositions in the system $\text{BaTiO}_3\text{-(CoFe}_2\text{O}_4)_{1-x}\text{(Co}_2\text{TiO}_4)_x$. The aggregates consist of piezoelectric BaTiO_3 crystals and the ferromagnetic $(\text{CoFe}_2\text{O}_4)_{1-x}\text{(Co}_2\text{TiO}_4)_x$ crystals both with their $\langle 001 \rangle$ direction parallel to the direction of their solidification. When this material is placed in a magnetizing field, the constituent $(\text{CoFe}_2\text{O}_4)_{1-x}\text{(Co}_2\text{TiO}_4)_x$ crystals deforms, causing a change in polarization of the neighboring BaTiO_3 crystals. Hulse *et al.*¹³⁾ obtained the crystalline aggregates by unidirectional solidification of the melts having the eutectic compositions in the $\text{Al}_2\text{O}_3\text{-ZrO}_2\text{(Y}_2\text{O}_3)$ system. The aggregates have a structure in which needle-like $\text{ZrO}_2\text{(Y}_2\text{O}_3)$ crystals, with their main crystallographic axis parallel to the direction of solidification, are dispersed uniformly in the Al_2O_3 matrix. Since the $\text{ZrO}_2\text{(Y}_2\text{O}_3)$ crystal has a larger thermal expansion coefficient than that of the Al_2O_3 crystal, a compressive stress is induced in the Al_2O_3 matrix when the solidified ingot is cooled to room temperature. Because of the existence of this micro-stress, the ingot thus obtained has a much higher mechanical strength than that of the conventional hot-pressed sintered alumina ceramics.

V. CONCLUSION

Compared with the other methods conventionally used for fabricating ceramics, the method of unidirectional solidification of the melts has some advantages; a) the ceramics consisting of unidirectionally oriented columnar crystals can be fabricated readily, b) the highly densified polycrystalline ceramics can be fabricated readily, and c) composite materials possessing special properties in a specified direction can be fabricated

readily from the melts of the eutectic compositions.

In spite of these special characteristics, this method has never been applied, in a large scale, to the industrial production of the polycrystalline oxide ceramics. The major technical reason is that, generally, the oxide crystals have low thermal conductivity and oxide melts have high viscosity near their melting temperature as compared with those of the metal crystals or melts: When the thermal conductivity of the crystal phase precipitated is low, it is difficult to set a steep temperature gradient in the melt near the crystal phase, and consequently cellular crystal growth and segregation are likely to occur. When the viscosity of the melt is high, it is difficult to suppress the formation of gas bubbles which remain in the ingot as small pores. It is hoped that further extensive studies on the relations between the solidification process and the microstructure of the resulting ingot will bring us new ideas for solving these difficulties.

ACKNOWLEDGMENTS

The authors acknowledge the technical assistance of Kunizo Tamaki, who performed a series of growth experiments, the results of which are incorporated in this article. Thanks also go to Sawako Matsumoto for her kind help in preparing the manuscript. The authors' work, the results of which are incorporated in the present article, was conducted partially with support of the Research Grant from the Ministry of Education, Japan.

REFERENCES

- (1) A. L. Stuijts, *Trans. Brit. Ceram. Soc.*, **55**, 57 (1956).
- (2) T. Takada, Y. Ikeda, H. Yoshinaga, and Y. Bando, Proc. Inter. Conf. Ferrite, 1970, p. 275.
- (3) M. H. Hodge, W. R. Bitler, and R. C. Bradt, *J. Amer. Ceram. Soc.*, **56**, 497 (1973).
- (4) T. Nishikawa, T. Nishida, K. Inoue, H. Inoue, and I. Uei, *Yogyo-Kyokai-Shi*, **82**, 241 (1974).
- (5) K. Kugimiya, E. Hirota, and Y. Bando, *IEEE Trans. Mag.*, **MAG-10** (3), 907 (1974).
- (6) T. Nishikawa, T. Nishida, and S. Sugimura, *Yogyo-Kyokai-Shi*, **83**, 110 (1975).
- (7) F. M. A. Carpay and W. A. Cense, *Scripta Metallurgica*, **8**, 11 (1974).
- (8) K. H. G. Ashbee, *J. Materials Sci.*, **10**, 911 (1975).
- (9) A. M. Alper, "Ceramic Microstructures", ed. R. M. Fulrath *et al.* John Wiley & Sons, New York, 1968, p. 763.
- (10) T. Noda, "Tanquesyo Ikusei Ho (Methods for Growing Single Crystals)," ed. Physical Society of Japan, Asakura, Tokyo, 1966, p. 343.
- (11) F. L. Kennard, R. C. Bradt, and V. S. Stubican, *J. Amer. Ceram. Soc.*, **56**, 566 (1973).
- (12) D. E. Harison, *J. Cryst. Growth*, **3**, **4**, 674 (1968).
- (13) C. Hulse and J. Batt, United Aircraft Research Laboratories Report, N910803-10, 1974.
- (14) D. Viechnicki and F. Schmid, *J. Materials Sci.*, **4**, 84 (1969).
- (15) F. Schmid and D. Viechnicki, *J. Materials Sci.*, **5**, 470 (1970).
- (16) F. L. Kennard, R. C. Bradt, and V. S. Stubican, *J. Amer. Ceram. Soc.*, **57**, 428 (1974).
- (17) F. Schmid and D. Viechnicki, "Advanced Materials, Composites and Carbon," Amer. Ceram. Soc. Inc., Ohio, 1971, p. 96.
- (18) S. Ito, T. Kokubo, and M. Tashiro, Abstracts of 13th Symposium on Basic Science of Ceramics, 1975, p. 4.
- (19) M. Arioka, T. Kokubo, and M. Tashiro, Abstracts of Annual Meeting of Ceramic Association of Japan, 1975, p. 38.
- (20) M. C. Flemings, "Solidification Processing", McGraw-Hill, New York, 1974, p. 58.
- (21) C. O. Hulse and J. A. Batt, "Advanced Material, Composites and Carbon", Amer. Ceram. Soc. Inc., Ohio, 1971, p. 132.

- (22) F. S. Galasso, W. L. Darby, F. C. Douglas, and J. A. Batt, *J. Amer. Ceram. Soc.*, **50**, 333 (1967).
- (23) D. J. Rowcliffe, W. J. Warren, A. G. Elliot, and W. S. Rothwell, *J. Materials Sci.*, **4**, 902 (1969).
- (24) G. Dhahenne, A. Revcolevschi, and R. Collongues, *Mater. Res. Bull.*, **7**, 1385 (1972).
- (25) J. Van Den Boomgaard, D. R. Terrell, R. A. J. Born, and H. F. J. I. Giller, *J. Materials Sci.*, **9**, 1705 (1974).
- (26) H. E. Labelle and A. I. MLavski, *Mater. Res. Bull.*, **6**, 571 (1971).
- (27) Idem, *ibid.*, **6**, 581 (1971).
- (28) B. Chalmers, "Principles of Solidification", John Wiley & Sons, New York, 1964, p. 260.
- (29) M. C. Flemings, "Solidification Processing", McGraw-Hill, New York, 1974, p. 94.
- (30) J. D. Hunt and K. A. Jackson, *Trans. Metal. Soc. AIME.*, **236**, 843 (1966).
- (31) S. Ito, T. Kokubo, and M. Tashiro, *Bull. Inst. Chem. Res., Kyoto Univ.*, **52**, 641 (1974).
- (32) B. Chalmers, "Principles of Solidification", John Wiley & Sons, New York, 1964, p. 186.
- (33) M. Cable, *J. Amer. Ceram. Soc.*, **49**, 436 (1966).
- (34) R. M. Glaister, *J. Amer. Ceram. Soc.*, **43**, 348 (1960).
- (35) S. Ito, T. Kokubo, and M. Tashiro, Abstracts of Annual Meeting of Ceramic Association of Japan, 1975, p. 68.
- (36) N. F. Borrelli, A. Herczog, and R. D. Maurer, *Appl. Phys. Letters*, **7**, 117 (1965).
- (37) C. H. Haertling and C. E. Land, *J. Amer. Ceram. Soc.*, **54**, 1 (1971).
- (38) G. S. Snow, *J. Amer. Ceram. Soc.*, **56**, 479 (1973).
- (39) A. M. J. G. Van Run, D. R. Terrell, and J. H. Scholing, *J. Materials Sci.*, **9**, 1710 (1974).